Eur. Phys. J. D **19**, 211–221 (2002)
DOI: 10.1140/epjd/e20020072

THE EUROPEAN PHYSICAL JOURNAL D
EDP Sciences

Electronic and geometric properties of alkali-C_{60} molecules

N. Hamamoto[a], J. Jitsukawa, and C. Satoko

Department of Physics, College of Humanities and Sciences, Nihon University 3-25-40 Sakura Jousui, Setagaya-ku, Tokyo 156-8550, Japan

Received 17 October 2001 and Received in final form 19 December 2001

Abstract. First-principle electronic structure calculations are carried out for $M_xC_{60}^q$, where M = Li, Na, K and $(x,q) = (1,0),(1,\pm1),(2,0),(3,-1),(6,0),(6,-1),(12,0)$ using the local density functional. The electric dipole moment for MC_{60} agrees with the experimental results. The calculated Mulliken charge indicates that the bonding of the alkali atom with C_{60} is mostly ionic except for lithium. The alkali atom prefers to make many bonds with the carbon atoms rather than a single bond with the neighbor carbon atom. The calculated adsorption energy suggest that the metal-metal bonding of sodiums and potassiums on C_{60} arises for more than the six valence electrons in the alkali atoms. The lithium-lithium bond is, on the other hand, not appeared for $x \leq 12$. The difference in the most stable geometry between lithiums and the other alkali atoms on C_{60} comes from the covalent character of the lithium-carbon bond.

PACS. 31.15.Ew Density-functional theory – 33.15.Dj Interatomic distances and angles – 33.15.Kr Electric and magnetic moments (and derivatives), polarizability, and magnetic susceptibility – 61.48.+c Fullerenes and fullerene-related materials

1 Introduction

After the discovery of superconductivity in K_3C_{60} films, alkali-doped fullerenes have much more interest in its variety of physical properties [1,2]. Works on the gas-phase exohedoral alkali-doped fullerenes have been devoted to predict the physical and chemical properties of the solid state fullerides [3–6]. An extensive experiment of the mass spectrum of $M_xC_{60}^+$ (M = Li, Na, K) clusters are performed by Martin *et al.* [3]. The observed high peak intensity at $Li_{12}C_{60}^+$ and $(K_6C_{60})_nK^+$ can be interpreted as the high stability of $Li_{12}C_{60}$ and K_6C_{60}, respectively. The even-odd alternation onset of $(Na_6C_{60})_nNa^+$ is regarded as the beginning of the metal-metal bonding on the C_{60} surface. They speculated that the first seven Na atoms transferring electrons to C_{60} are placed themselves as far from one another as possible. After the seventh Na atom adsorption on C_{60}, an eighth Na atom joins one of the Na^+ ions on C_{60}, and a ninth Na atom form a Na_3^+ trimer ion. The ionic nature of bonding for the K atoms with C_{60} is also suggested in the photoelectron spectroscopy (PES) study of $K_xC_{60}^-$ ($x = 0$ to 3) performed by Wang *et al.* [6].

A systematic PES study of Palpant *et al.* gives the vertical detachment energy (VDE) and the adiabatic electron affinity (AEA) for $Na_xC_{60}^-$ ($x = 0{-}33$) [4,5]. Based on the peak positions of VDE and AEA at $x = 3,6,9,12$, they proposed special stability of the trimers on C_{60}. A single sodium trimer on C_{60}, however, disagrees with the growth sequence proposed by Martin *et al.* It is also impossible to identify the geometry of these clusters by the photoelectron or the mass spectrum data. Then, the theoretical electronic structure calculation is necessary to determine the most stable geometry of these molecules.

Many articles have been devoted to the theoretical calculations of alkali fullerides [7–15]. The stable geometries of LiC_{60} [10], NaC_{60} [12], and KC_{60} [14], are examined using the Hartree-Fock calculations. Kohanoff *et al.* applied the Car-Parrinello method within the local density approximation [9]. They find that the icosahedral $Li_{12}C_{60}$ cluster is stable. The results of the unrestricted Hartree-Fock (UHF) calculation for Na_2C_{60} performed by Hira and Ray show that the sodium dimer is placed perpendicular to the long bridge of C_{60} in the most stable geometry [13]. The structure for K_2C_{60} and K_3C_{60} were examined by Weis *et al.* [14] using the restricted open shell Hartree-Fock formalism.

The UHF calculation of Li_xC_{60} performed by Aree *et al.* is extended into the number of the Li atoms $x = 1$–6, 12 [11]. The applications of the semi-empirical modified-neglect-of-diatomic-overlap (MNDO) quantum chemical calculations [15] for Li_xC_{60} provides the most stable configuration for the large number of the Li atoms ($x \leq 14$). However, the semi-empirical method MNDO sacrifices some of accuracy compared with the first-principle calculations. Moreover, these calculations are performed with the assumption of symmetry restriction on the geometry of molecule. In the restricted symmetry calculations, the initial positions and the geometries of the clusters are quite limited. The assumption of symmetry restriction is, therefore, inadequate to investigate the geometry speculated by

[a] e-mail: hamamoto@phys.chs.nihon-u.ac.jp

the experiments such as the trimers of the alkali atoms on fullerene. To provide these geometries using the theoretical calculation, we should remove the symmetry restriction for the geometry of the clusters.

The number of the alkali atoms on C_{60} in the above calculations is restricted from one to three for Na_xC_{60} and K_xC_{60}. However, the interesting bonding features of the alkali atoms on C_{60} are speculated for more than the two alkali atoms on C_{60}. For example, the sodium trimer on C_{60} are speculated from the experiment. The strong stability are suggested for the K_6C_{60} and the $Li_{12}C_{60}$ clusters. The Na–Na bonding on C_{60} appears when the number of valence electrons is larger than 6. Therefore, the calculation for more than the three alkali atoms on C_{60} are needed to compare the character of bonding between lithiums, sodiums, and potassiums on C_{60}.

The purpose of the present study is to investigate the bonding nature of M_xC_{60} using the geometry optimization calculation in the density functional theory without any symmetry restrictions. We will refer to the alkali atoms Li, Na, and K as the symbol M throughout the paper. We performed the calculation for $M_xC_{60}^q$, $(x,q) = (1,0),(1,\pm1),(2,0),(3,-1),(6,0),(6,-1),(12,0)$ in which the interesting features on bonding are speculated from the experiment. The calculated most stable geometries and the Mulliken charges for these molecules are presented in this paper.

2 Method

We performed self-consistent field calculations for M_xC_{60} using the density functional theory (DFT). The calculations were carried out using Amsterdam Density Functional program system (ADF) [16] which is a DFT code using the linear combination of atomic orbitals (LCAO) approach together with Slater type atomic orbitals. The bases set used in the calculations is the double-zeta bases set. In this work, we applied the local density approximation (LDA) using the exchange-correlation potential of Vosko, Wilk, and Nusair [17].

We performed the geometry optimization of M_xC_{60} which is divided into two steps. First, geometry of C_{60} is optimized without any symmetry constraint. The carbon atoms in the geometry optimized C_{60} are located near the I_h symmetric position of C_{60}. Two kinds of CC bond lengths in C_{60} are obtained as C=C = 1.384 Å and C–C = 1.435 Å. The deviation of the C–C and the C=C bonds in C_{60} from the averages are less than 0.002 Å. They are good agreement with the electron diffraction data of 1 003 K gas phase C_{60} [18] (C=C = 1.401 Å and C–C = 1.458 Å). The present method produces the bond lengths with the same level of accuracy as the MP2 results [19] (C=C = 1.406 Å and C–C = 1.446 Å). The HOMO-LUMO energy gap of C_{60} is obtained as 1.67 eV which is consistent with the photoelectron spectroscopy experiment of C_{60}^- [20] (1.5–2.0 eV). We obtained five fold degenerate HOMO which corresponded to h_u of the icosahedral group I_h. The three fold degenerate LUMO is regarded as t_{1u} of icosahedral group. The three fold degenerate level 1.12 eV above the LUMO is specified as t_{1g} of icosahedral C_{60}. In the next step, we performed the geometry optimization of M_xC_{60} without any symmetry constraint. In order to save computer work, we assumed the position of C_{60} to be fixed to the geometry obtained in the first step.

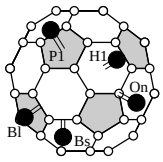

Fig. 1. The five types of initial geometry for MC_{60}.

In order to check this assumption, we performed the geometry optimization of NaC_{60}^- with being allowed to move all the C atoms and the Na atoms. The NaC, the C–C, and the C=C bond length are changed within 0.02 Å from the result of the calculation using the assumption. The total energy is 0.088 eV lower than the result of optimization fixing the position of C_{60}. We believe that this small deviation of the total energy do not affect the relative values of the total energy for M_xC_{60} in different geometries.

3 Results

In this section, we will show the result of the geometry optimization calculation of M_xC_{60}. In Section 3.1, the adsorption of a single alkali atom to C_{60} is discussed. The nature of adsorption of many alkali atoms to C_{60} is summarized in the beginning of Section 3.2. More detailed descriptions of the results for $x = 2, 3, 6, 12$ are given in the following subsections. Throughout the following sections, we use the adsorption energy ΔE which is defined as

$$\Delta E \equiv E(C_{60}^q) + xE(M) - E(M_xC_{60}^q), \qquad (1)$$

where $E(X)$ is the total energy of molecule X and q is the ionicity $(0, \pm1)$.

3.1 Adsorption of single alkali atom on C_{60}

Five types of initial geometry are selected for the calculation of MC_{60}^q. As shown in Figure 1, the initial positions of the alkali atom are above the center of the pentagonal ring (P1), above the center of the hexagonal ring (H1), and above the carbon atom (On). There are two kinds of geometries, Bl and Bs, that is, the alkali atom is located above the center of the long bridge between the hexagonal and the pentagonal ring (Bl) and the short bridge between the hexagonal rings (Bs), respectively. In Table 1, we show the adsorption energies ΔE and the Mulliken's gross charges on the alkali atom [21] for the five types of the optimized geometries. In the geometry optimization for the Bl, the Bs, and the On geometry, we allow to move the alkali atoms along the axis which connects the

Table 1. The adsorption energies ΔE (in eV) and the Mulliken charges of the alkali atom (in electrons) for MC_{60}^q, (M = Li, Na, K, $q = 0, \pm 1$) of the five types of geometries.

	P1		H1		Bs		Bl		On	
	ΔE	Charge	ΔE	Charge	ΔE	Charge	ΔE	Charge	ΔE	Charge
LiC_{60}^-	1.965	+0.836	1.943	+0.840	1.747	+0.842	1.606	+0.885	1.423	+0.897
LiC_{60}	2.414	+0.908	2.388	+0.901	2.258	+0.925	2.087	+0.942	2.202	+0.947
LiC_{60}^+	4.352	+0.968	4.305	+0.954	4.123	+0.984	4.025	+0.989	4.264	+0.990
NaC_{60}^-	1.438	+0.998	1.490	+1.025	1.076	+1.009	1.082	+1.041	1.048	+0.969
NaC_{60}	2.052	+1.057	2.101	+1.067	1.930	+1.054	1.782	+1.060	1.983	+1.040
NaC_{60}^+	4.180	+1.097	4.191	+1.100	4.138	+1.075	4.131	+1.077	4.125	+1.075
KC_{60}^-	1.466	+1.069	1.534	+1.080	1.195	+1.031	1.249	+1.041	1.224	+1.046
KC_{60}	2.339	+1.093	2.369	+1.095	2.081	+1.056	2.109	+1.064	2.083	+1.056
KC_{60}^+	4.696	+1.104	4.677	+1.109	4.635	+1.072	4.613	+1.074	4.604	+1.081

center of C_{60} with the center of the long bridge, the center of the short bridge, and the carbon atom, respectively.

Our results show that the P1 and the H1 geometry are the most stable geometry for lithium and the other alkali atoms, respectively. The differences of adsorption energy between the geometries P1, H1 and the other geometries are lower than 0.5 eV for all kinds of alkali atoms. Some results of our calculation agree with the previous works performed using the different methods. The most stable geometry of neutral KC_{60} is the H1 geometry, which is consistent with the result of the restricted open-shell Hartree-Fock calculation [14]. For NaC_{60}^+, the H1 geometry is the most stable geometry, which agrees with the result of the unrestricted Hartree-Fock calculation performed by Hira and Ray [12].

The most stable geometry is the P1 geometry for LiC_{60}^q ($q = 0, \pm 1$). The adsorption energy of the P1 geometry is 0.04 eV higher than that of the H1 geometry which gives the second highest adsorption energy. For NaC_{60}^+ and NaC_{60}, the H1 geometry is the most stable geometry. The energy differences between the H1 geometry and the secondly most stable P1 geometry are not significantly large (≤ 0.03 eV).

These small energy differences sometimes result in the inconsistency between the different methods. In fact, the H1 geometry is the most stable geometry according to the calculation of LiC_{60} performed by Zimmermann *et al.* [10]. In the UHF calculation of neutral NaC_{60} performed by Hira and Ray [12], they obtained the five types of stable geometries which are the same as the geometries selected for the present calculation. Their results show no energy differences between the adsorption energies for the different types of these geometries.

The Mulliken population analysis [21] is used to investigate the bonding nature. We calculated the Mulliken's subtotal gross populations in MO ψ_i on the alkali atoms ($Q_{\rm A}^i$) and on the carbon atoms ($Q_{\rm C}^i$). The Mulliken's subtotal overlap population in MO ψ_i between the alkali atoms and the carbon atoms ($O_{\rm AC}^i$) is also evaluated. In Figure 2, we show the densities of populations $Q_{\rm A}(E)$, $Q_{\rm C}(E)$, and $O_{\rm AC}(E)$ which are defined as

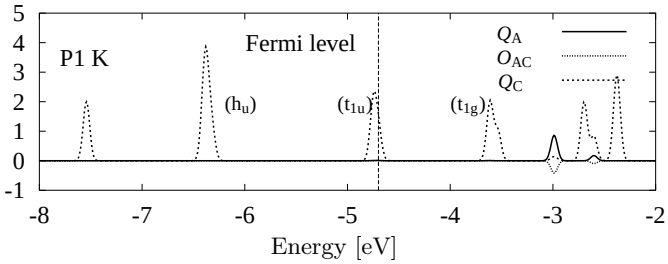

Fig. 2. The density of the Mulliken population for the potassium atom and the carbon atom $Q_{\rm A}(E)$, $Q_{\rm C}(E)$, the overlap population between the potassium atom and the carbon atom $O_{\rm AC}(E)$ of KC_{60} for the P1 geometry. The smearing parameter $\sigma = 4.5 \times 10^{-2}$.

the corresponding populations smeared by the Gaussian function $F(x) = \exp(-x^2/\sigma^2)$,

$$Q_{\rm X}(E) = \sum_i Q_{\rm X}^i F(E - \epsilon_i),$$
$$O_{\rm XY}(E) = \sum_i O_{\rm XY}^i F(E - \epsilon_i), \qquad (2)$$

where ϵ_i is the eigenvalue of energy for the molecular orbital ψ_i. Since the populations are not significantly changed for the different geometries and the kinds of alkali atoms, we show the populations only for the P1 geometry of KC_{60}.

The small overlap population between the alkali atom and the carbon atoms ($O_{\rm AC}$) in Figure 2 represents the small mixing of these orbitals. The molecular orbitals of KC_{60} can be divided into two types. One originates from the carbon atoms and the other is mainly constructed from the alkali atom. The approximately 3 fold degenerate Fermi level corresponds with the t_{1u} orbital of C_{60}. The nearly 5 fold and the approximately 3 fold degenerate levels in the lower and the higher energy sides of the Fermi level are originated from the h_u and the t_{1g} orbital of C_{60}, respectively. The levels constructed mainly from the alkali atom are located above the t_{1g} orbital.

Table 2. The calculated dipole moment in debye. The experimental results are tabulated in the right column [23].

C_{60}	P1	H1	Bs	Bl	On	Experiment
LiC_{60}	11.62	10.71	13.72	13.77	14.66	12.4 ± 2.0
NaC_{60}	15.80	14.63	16.54	16.48	17.10	16.3 ± 1.6
KC_{60}	18.89	18.49	19.57	19.10	19.81	21.5 ± 2.2

The molecular orbital constructed mainly from the alkali atom is unoccupied for the P1 geometry. It suggests the charge transfer from the alkali atom to the t_{1u} orbital of C_{60}. The Mulliken charges presented in Table 1 are approximately equal to 1.0 for all kinds of the alkali atoms, which indicates almost complete transfer of an electron, in other words, the ionic bonding of the alkali atom to C_{60}. The Mulliken charges are slowly increased in the series of the heavier alkali atoms, lithium, sodium, potassium. This increasing behavior can be explained from the valence orbital energy of the alkali atom. The calculated energies of the valence s orbital of the Li, the Na, and the K atom are calculated as -3.02, -2.84, and -2.54 eV, respectively.

Our calculation gives reasonable results in the electric dipole moment which can be directly compared with the results of the experiment [22,23]. The dipole moment of MC_{60} is collected in Table 2. The calculated dipole moment of each geometry is increased continuously from lithium to potassium. This behavior is consistent with the results of optimized geometries and the Mulliken charges of the alkali atoms. The Mulliken charge of the alkali atom and the distance from the center of C_{60} to the position of the alkali atom increase continuously from lithium to potassium.

The calculated dipole moment for the H1 (On) geometry is the smallest (largest) of those of the five types of geometries independent of the kinds of alkali atoms. The result is explained by the smallest (longest) length between the position of the alkali atom and the center of C_{60} obtained for the H1 (On) geometry.

The average value of the dipole moment for MC_{60} is extracted by the molecular beam deflection experiment [22,23]. Since the temperature is high enough for the alkali atoms to be able to move freely over the surface of the C_{60} cage, the extracted moment can be regarded as an average of the dipole moment. Although some dipole moment in Table 2 do not agree with the experimental results, our calculation gives reasonable results as an average of the dipole moment.

Table 3 shows the bond length between the alkali atom and the nearest carbon atom. We can find in Table 3 that the bond length for the On geometry is shorter than that of any other geometries. The MC bond lengths in the On geometry for neutral MC_{60} are nearly equal to the bond length of a free MC molecule which are 2.00, 2.35, and 2.62 Å for lithium, sodium, and potassium, respectively. The calculated bond lengths become short when the charge of MC_{60} are decreased. The bond length of MC_{60}^{-} are shorter than that of MC_{60} and MC_{60}^{+} in the same geometry. This result indicates that the bond length is determined by the number of the HOMO valence electrons.

Table 3. The distances between the alkali atom and the nearest carbon atom for the five types of geometries. The values are given in Å.

	P1	H1	Bs	Bl	On
LiC_{60}^{-}	2.23	2.28	2.10	2.14	2.00
LiC_{60}	2.30	2.32	2.19	2.18	2.08
LiC_{60}^{+}	2.39	2.44	2.27	2.24	2.18
NaC_{60}^{-}	2.60	2.58	2.39	2.37	2.29
NaC_{60}	2.70	2.69	2.47	2.46	2.39
NaC_{60}^{+}	2.79	2.77	2.64	2.66	2.53
KC_{60}^{-}	2.88	2.95	2.74	2.66	2.59
KC_{60}	2.98	3.03	2.82	2.76	2.69
KC_{60}^{+}	3.07	3.13	2.99	3.00	2.77

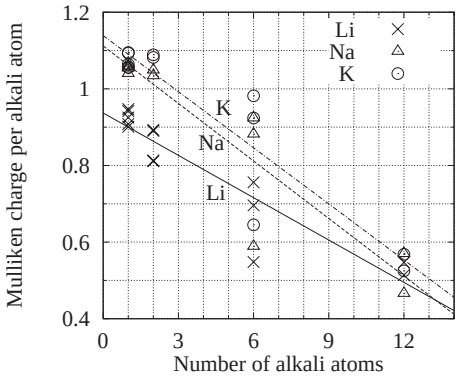

Fig. 3. The Mulliken charges per alkali atom (in electrons) in M_xC_{60} as a function of x.

The bond length between the alkali atom and the nearest carbon atom becomes longer according as the number of the nearest carbon atoms is increased. When the number of the nearest carbon atoms is increased, the covalent bond per carbon atom becomes weak. In spite of the weak bond, we obtained the highest adsorption energy for the H1 and the P1 geometry in which the number of the nearest carbon atoms is the largest and the second largest of five types of geometries, respectively. We find that the alkali atom prefers to make many bonds with the nearest carbon atoms rather than a single strong bond.

3.2 Adsorption of many alkali atoms on C_{60}

In this subsection we discuss the bonding nature of the alkali atoms on C_{60}. Figure 3 shows the Mulliken charges per alkali atom of M_xC_{60} ($x = 1, 2, 6, 12$) for various geometries shown in Figures 1 and 6. If many alkali atoms are lying on C_{60}, we take their average over each alkali atom. The lines in the figure are obtained by the linear least square fit to the data for each kind of alkali atom.

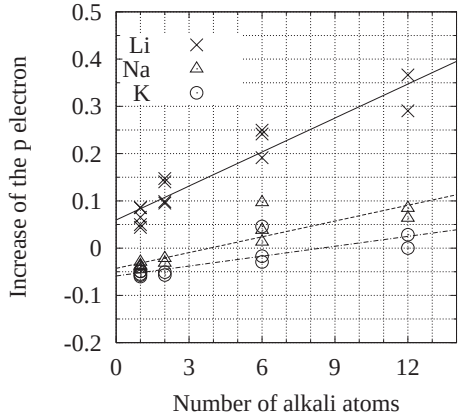

Fig. 4. Increase of the p electron population per alkali atom in M_xC_{60} as a function of x.

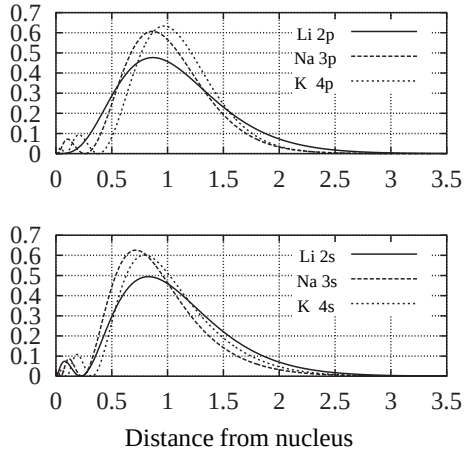

Fig. 5. The radial distribution function of the atomic orbitals as a function of the distance from the nucleus scaled by the M−C distance. The M−C distance is taken as 2.00, 2.35, and 2.62 Å for Li, Na, and K, respectively.

We find from Figure 3 that the Mulliken charges are decreased for all kinds of the alkali atoms according as the number of the alkali atoms is increased. The lines in the figure indicates that the Mulliken charges of sodium and potassium behave similar as a function of the number of the alkali atoms. The charges of lithium are smaller than those of sodium and potassium for all number of the alkali atoms we investigated. The decrease of the Mulliken charges for larger number of the alkali atoms result from the more covalent character of bonding between the lithium atom and the carbon atom, which is also true for the alkali-graphite intercalation [24] and organolithium compounds [25]. The enhanced covalency in lithium-carbon interaction comes from the contribution of the $2p$ electrons of the lithium atom.

To investigate the contribution of the p electrons in the alkali atom, we calculated the Mulliken's total gross population in atomic p orbitals of an atom X; $q_{X(p)}$ [21]. In Figure 4, we plotted the increase of the population in atomic p orbitals of an alkali atom $\Delta q_{A(p)}$,

$$\Delta q_{A(p)} = q_{A(p)} - N_p, \tag{3}$$

where N_p means the number of the p electrons in a free single atom. If many alkali atoms are lying on C_{60}, we take their average. We find from Figure 4 that the population of the valence p electrons of lithium is large compared with that of the other alkali atoms. The lines in the figure is obtained by the linear least square fit to the data for each kind of alkali atom.

The large contribution of the $2p$ atomic orbital in the lithium-carbon bonding comes from the character of the Li atom. The polarizability of the alkali atom divided by the volume of an atom can be a measure for the p contribution in the external electric field caused by the neighbor carbon atom. The polarizability measured by the experiment, 24.0, 24.4, and 41.3 $Å^3$ [26], divided by the cube of the atomic radius 1.56, 1.91, and 2.35 Å [27], are obtained as 6.31, 3.50, and 3.18 for the Li, the Na, and the K atom, respectively. The large value for the Li atom is consistent with the large p contribution of the lithium-carbon bonding in the present calculation.

In Figure 5, we show the radial distribution function of the atomic orbitals for the alkali atoms as a function of the distance from the nucleus scaled by the M−C distance. The M−C distances are taken as 2.00, 2.35, and 2.62 Å for the Li, the Na, and the K atom, respectively. The $2s$ and the $2p$ orbital of the Li atom is more diffused compared with the valence orbitals of the Na and the K atom. The diffuse orbital arises the larger overlap between the atoms, which enhance the covalent character of bonding between the atoms. Furthermore, the valence p orbital energy of the Li atom is −1.14 eV which is smaller than that of the Na and the K atom, −0.43 and −0.63 eV, respectively. The small energy difference between the valence orbital of the alkali atom and that of the carbon atom leads the covalent bonding between them.

The nature of the bonding between the alkali atoms is related to the Mulliken charge of the alkali atom. If all valence electrons in the alkali atoms are transfered to C_{60}, interaction between the alkali cations will be repulsive due to the Coulomb repulsive force. We expect that the alkali atoms are located as far from each other as possible for the most stable geometry. On the other hand, if the valence electrons are not completely transfered to C_{60}, the interaction between the alkali atoms will be less repulsive. We can expect that the alkali atoms prefer to be located in close position together on the C_{60} surface because of the valence electrons in the bonding molecular orbital between the alkali atoms. In the experimental work [3,4], the alkali atom trimers on C_{60} is speculated as the most stable geometry. Since the Mulliken charge is decreased for larger number of the alkali atoms, these geometry may be possible. The discussion about the most stable geometry will be presented in the following subsections.

3.2.1 M_6C_{60}

We first discuss the bonding nature of M_6C_{60} and $M_6C_{60}^-$ which have six and seven valence electrons, respectively.

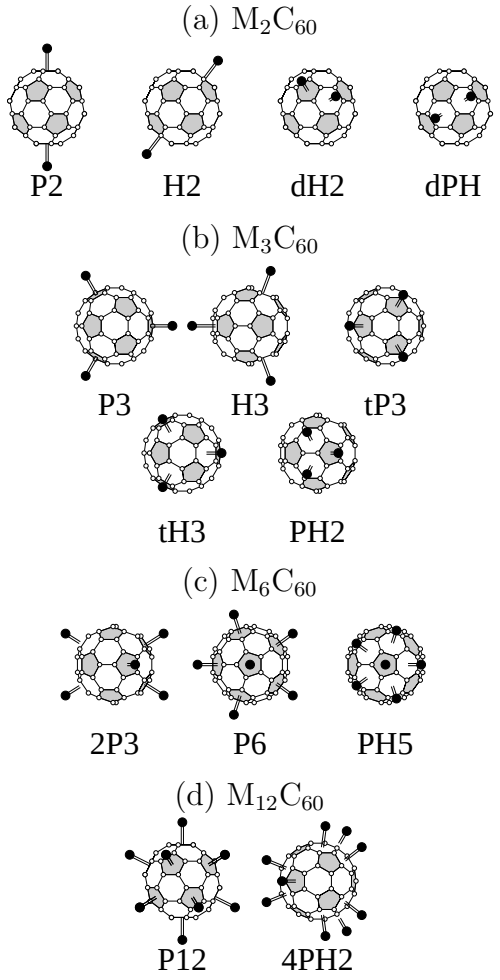

Fig. 6. The selected geometries for M_xC_{60} of $x = 2$ (a), 3 (b), 6 (c), and 12 (d). The black circles represent the alkali atoms and the white ones are the carbon atoms.

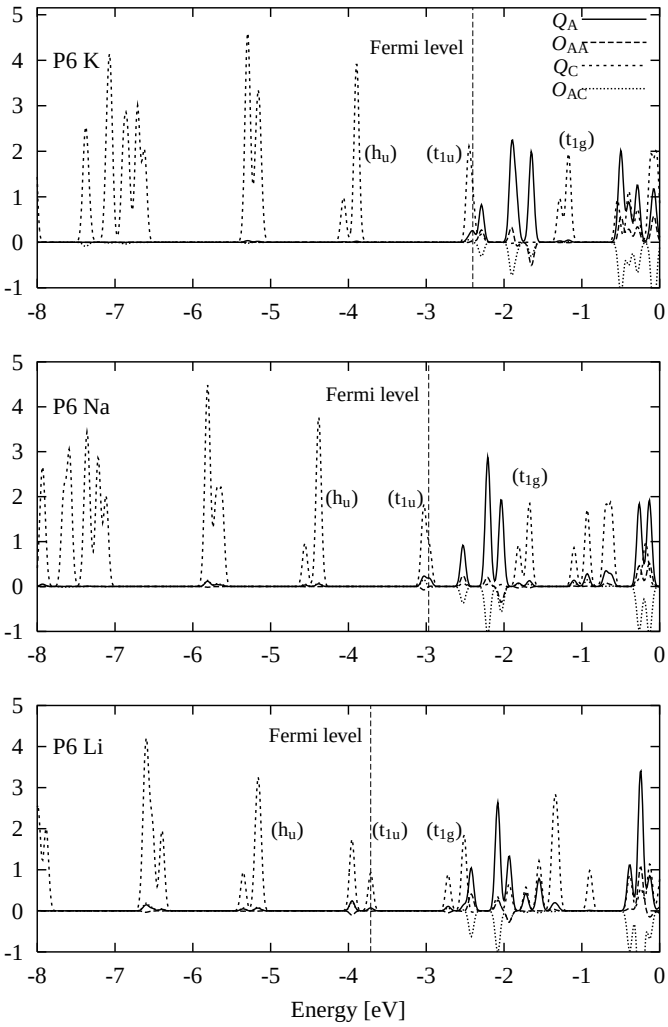

Fig. 7. The density of the Mulliken population of the alkali atom ($Q_A(E)$) and the carbon atom ($Q_C(E)$), the overlap population between the alkali atoms ($O_{AA}(E)$), between the alkali atom and the carbon atom ($O_{AC}(E)$) for M_6C_{60} of the P6 geometry are illustrated. The upper, the middle, and the lower figure correspond to K_6C_{60}, Na_6C_{60}, and Li_6C_{60}, respectively. The smearing parameter $\sigma = 4.5 \times 10^{-2}$.

Since the adsorption energies of the P1 and the H1 geometry are smaller than the other geometries in the adsorption of a single alkali atom, we restrict the initial positions of the alkali atoms in M_xC_{60} to the positions above the pentagonal ring or the hexagonal ring. We obtain the result for three types of geometries which are named as P6, PH5, and 2P3. The initial positions of the alkali atoms for each geometry are illustrated in Figure 6c. In the P6 geometry, the alkali atoms are located above the pentagonal rings of which the positions are as close to one another as possible. In the PH5 geometry, one of the alkali atoms is located above the pentagonal ring. The others are located above the hexagonal rings surrounding this pentagonal ring. In the 2P3 geometry, the three alkali atoms are placed above the three pentagonal rings located in contact with the same hexagonal ring. The three alkali atoms and the other three alkali atoms are placed at the opposite positions of C_{60}.

In the optimized geometry of P6, the shortest distances between the alkali atoms are 5.42, 5.99, and 6.32 Å for Li_6C_{60}, Na_6C_{60}, and K_6C_{60}, respectively. The distance in the optimized geometry of PH5 are 3.39, 3.67, and 4.11 Å for Li_6C_{60}, Na_6C_{60}, and K_6C_{60}, respectively. The results of the distance between the alkali atoms for the PH5 geometry are approximately equal to the twice of the atomic radius which are 3.12, 3.82, and 4.70 Å for the Li, the Na, and the K atom, respectively. We expect, therefore, that the bonding between the alkali atoms is weak for the P6 geometry and strong for the PH5 geometry.

Figure 7 shows the densities of the Mulliken populations $Q_A(E)$, $Q_C(E)$ and the densities of the overlap populations $O_{AA}(E)$, $O_{AC}(E)$ for M_6C_{60} of the P6 geometry, where $O_{AA}(E)$ means the Mulliken's subtotal overlap population in MO ϕ_i between the alkali atoms (O^i_{AA}) smeared by the Gaussian function (see Eq. (2)). The same quantities of the PH5 geometry are shown in Figure 8. In Figure 7, the three peaks of Q_A located around -2 eV are constructed mainly from the valence s orbital of the six alkali atoms. The lowest energy peak of the three peaks

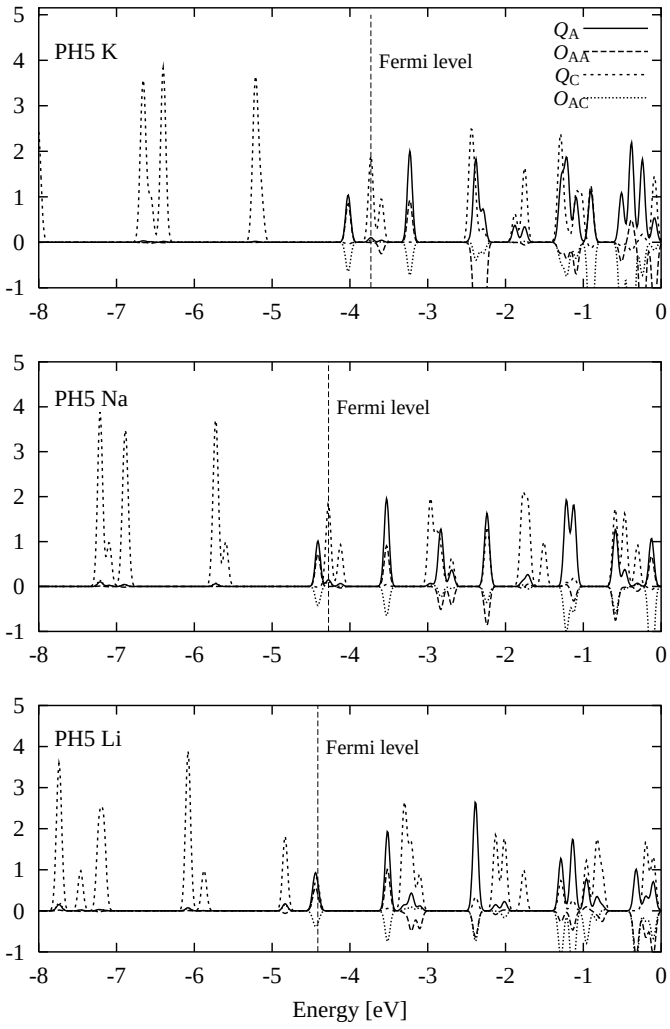

Fig. 8. The density of the Mulliken population of the alkali atom ($Q_A(E)$) and the carbon atom ($Q_C(E)$), the overlap population between the alkali atoms ($O_{AA}(E)$), between the alkali atom and the carbon atom ($O_{AC}(E)$) for M_6C_{60} of the PH5 geometry are illustrated. The upper, the middle, and the lower figure correspond to K_6C_{60}, Na_6C_{60}, and Li_6C_{60}, respectively. The smearing parameter $\sigma = 4.5 \times 10^{-2}$.

have weak bonding character, and the other two peaks have antibonding character. Less than the 0.3 eV energy differences between these peaks indicate the small overlap between the atomic valence orbitals of the alkali atoms. In Figure 8, there are the corresponding three peaks which spread out in the wide energy region between −4.4 eV and −2.2 eV, because of the increasing overlap between the valence orbitals of the alkali atoms. We named the lowest energy orbital of these three orbitals as "*s*-dominant bonding orbitals" which are found as the Q_A peak positions at −2.4, −2.5, and −2.3 eV in Figure 7 and −4.5, −4.5, −4.0 eV in Figure 8 for lithium, sodium, and potassium, respectively.

Which of the PH5 and the P6 geometry is more stable is determined by the metal-carbon interaction and the metal-metal interaction. We find from Figure 8 that the

Table 4. The adsorption energies ΔE (in eV) and the Mulliken charges per alkali atom (in electrons) for M_6C_{60} and $M_6C_{60}^-$.

	2P3		P6		PH5	
	ΔE	Charge	ΔE	Charge	ΔE	Charge
Li_6C_{60}	14.20	+0.756	14.40	+0.696	11.93	+0.548
Na_6C_{60}	10.75	+0.924	10.47	+0.882	9.58	+0.589
K_6C_{60}	10.98	+0.982	10.59	+0.924	10.05	+0.645
$Li_6C_{60}^-$	11.44	+0.667	11.96	+0.561	11.11	+0.445
$Na_6C_{60}^-$	8.20	+0.734	8.20	+0.704	8.24	+0.497
$K_6C_{60}^-$	7.25	+0.702	7.17	+0.666	8.41	+0.589

s-dominant bonding orbital is occupied in the PH5 geometry. The negative overlap O_{AC} in the *s*-dominant bonding orbital represents the antibonding character of the alkali atoms with C_{60}. When the *s*-dominant bonding orbital are occupied, the metal-metal bond arises in compensation for the weak metal-carbon bond. On the other hand, the P6 geometry is stabilized by the metal-carbon bonding. The instabilization caused by the weak metal-carbon interaction and the stabilization due to the metal-metal interaction determine whether the PH5 geometry is stable rather than the P6 geometry. The result of the calculation for the adsorption energy presented in Table 4 shows that the P6 geometry is stable compared with the PH5 geometry for all kinds of alkali atoms. The adsorption energies of Li_6C_{60}, Na_6C_{60}, and K_6C_{60} for the P6 geometry are 2.47, 0.89, and 0.54 eV higher than those of the PH5 geometry, respectively.

We find from Figure 7 that the Fermi level is constructed from the t_{1u} orbital of C_{60}. The main components of the LUMO of Na_6C_{60} and K_6C_{60} for the P6 geometry are considered to be the *s*-dominant bonding orbital, while the LUMO of Li_6C_{60} is the orbital composed of t_{1g} orbital of C_{60}. For $Na_6C_{60}^-$ and $K_6C_{60}^-$, the seventh valence electron occupies the *s*-dominant bonding orbital. Since the electrons in the *s*-dominant bonding orbital is considered to be occupied both in P6 and in PH5, the bonding of the alkali atom to the carbon atom is weak. The PH5 geometry is, therefore, expected to be the most stable geometry because the alkali atoms make stronger bond in the PH5 geometry compared with the P6 geometry. The adsorption energy and the Mulliken charge of the alkali atom of $M_6C_{60}^-$ are shown in Table 4. Actually, the most stable geometry is the PH5 geometry for $Na_6C_{60}^-$ and $K_6C_{60}^-$, while P6 is the most stable geometry for $Li_6C_{60}^-$. Similar values are obtained for the adsorption energies of $Na_6C_{60}^-$ for the different geometries, which is also true for Na_6C_{60}. The most stable geometry is, however, changed to the PH5 geometry. For $K_6C_{60}^-$, we find a large difference of the adsorption energy between the PH5 geometry and the other geometries (1 eV).

We find from Table 4 that the Mulliken charges of the P6 geometry are increased from Li_6C_{60} to K_6C_{60}. The lowest Mulliken charge for Li_6C_{60} is caused by the covalency of the Li atom with the C atom. In fact, we find

Table 5. The adsorption energies ΔE (in eV) and the Mulliken charges per alkali atom (in electrons) of M_2C_{60}.

	P2		H2		dH2		dPH	
	ΔE	Charge	ΔE	Charge	ΔE	Charge	ΔE	Charge
Li_2C_{60}	4.821	+0.893	4.777	+0.890	4.354	+0.811	4.367	+0.813
Na_2C_{60}	3.971	+1.034	4.094	+1.049				
K_2C_{60}	4.408	+1.082	4.519	+1.089				

from Figure 7 that the mixing of the C_{60} molecular orbital with the atomic orbital of the alkali atom is increased from K_6C_{60} to Li_6C_{60}. For example, the peak corresponding to the h_u orbital is constructed mostly from Q_C, but there is a small peak of Q_A at the same energy. The height of this small peak of Q_A for Li_6C_{60} (0.07) is more decreased for Na_6C_{60} (0.06) and K_6C_{60} (0.02).

We find from Q_C of Figures 7 and 8 that the energies of the molecular orbital mostly composed of the carbon atomic orbital for K_6C_{60} are higher than that of Li_6C_{60} and Na_6C_{60}. For example, the peak of Q_C located around -4.0 eV for K_6C_{60} of the P6 geometry is shifted to -4.5 eV and -5.3 eV for Na_6C_{60} and Li_6C_{60}, respectively. This energy shift can be explained by the large amount of charge transfer from the K atom to C_{60}.

As mentioned previously, the PH5 geometry is the most stable geometry for $Na_6C_{60}^-$ and $K_6C_{60}^-$ because of the seventh electron in the s-dominant bonding orbital, while the P6 geometry becomes the most stable geometry for $Li_6C_{60}^-$. This is explained by the position of the t_{1g} orbital in Figure 7, that is, the t_{1g} level of Li_6C_{60} located lower than the s-dominant bonding orbital is shifted to the higher position than the s-dominant bonding orbital in Na_6C_{60} and K_6C_{60}. The t_{1g} orbital energy shift is also explained by the charge transfer from the alkali atom to C_{60}, in other words, the covalency of the metal-carbon interaction. Therefore, the t_{1g} orbital located lower than the s-dominant orbital, which is the origin the most stable P6 geometry in $Li_6C_{60}^-$, is caused by the enhanced covalency of lithium-carbon interaction.

3.2.2 M_2C_{60}

The four types of geometries considered for M_2C_{60} are named as P2, H2, dH2, and dPH which are represented in Figure 6a. For the P2 (H2) geometry, the two alkali atoms are placed above the pentagonal (hexagonal) rings which are located at the opposite sides of C_{60}. In the dH2 (dPH) geometry, the initial positions of the alkali atoms are above the hexagonal ring and the neighboring hexagonal (pentagonal) ring.

Table 5 shows the adsorption energy and the Mulliken charge per alkali atom for the four types of initial geometries. We find that P2 and H2 are the most stable geometry for lithium and the other alkali atoms, respectively. For K_2C_{60}, the most stable geometry is consistent with the result of the Hartree-Fock calculation [14]. The present results do not consistent with the results of the Hartree-Fock calculation for Li_2C_{60} [11] in which H2 is the most stable geometry. However, the small difference between the adsorption energies of the H2 and the P2 geometry (0.03 eV) may lead different geometries within the DFT or the Hartree-Fock level calculations.

The adsorption energies of the H2 and the P2 geometry are 0.1–0.3 eV lower than the twice of those of the H1 and the P1 geometry. The Mulliken charges for the P2 (H2) geometry are not significantly different from those of the P1 (H1) geometry of MC_{60}. The optimized geometry can not be obtained for the dH2 and the dPH geometry of Na_2C_{60} and K_2C_{60}, because these geometries are far away from the stable positions of a sodium and a potassium dimer on C_{60}. The adsorption energies of the dH2 and the dPH geometry for Li_2C_{60} are lower than those of the P2 and the H2 geometry. The alkali atoms, therefore, prefers to be located as far from each other as possible because of the repulsive Coulomb interaction between the alkali atoms in M_2C_{60}.

3.2.3 M_3C_{60}

Five types of initial geometries considered for M_3C_{60} are named as P3, H3, tP3, tH3, and PH2, which are illustrated in Figure 6b. For the P3 and the H3 geometry, the positions of the three alkali atoms are placed above the pentagonal and the hexagonal rings, respectively. The pentagonal and the hexagonal rings are located as far from one another as possible. For the tP3 and the tH3 geometries, the three alkali atoms are placed above the pentagonal and the hexagonal rings, respectively. Each pentagonal and hexagonal ring is located in contact with the same hexagon. For the PH2 geometry, one alkali atom is placed above the pentagonal ring, the other two alkali atoms are located on the neighboring hexagonal rings. The pentagonal ring is in contact with these two hexagonal rings.

The calculated adsorption energies and the Mulliken charges are collected in Table 6. For $M_3C_{60}^-$, the highest adsorption energy is obtained as tP3, P3, and H3 for Li_3C_{60}, Na_3C_{60}, and K_3C_{60}, respectively. The adsorption energy of the most stable geometry is almost same as the sum of the adsorption energy of the P1 or the H1 geometry, which indicates the negligible contribution of the metal-metal bond. The higher Mulliken charge of an alkali atom is obtained when the average distance between the alkali atoms are longer. For all of the alkali atoms, the maximum charge is achieved at the P3 or the H3 geometry and the minimum charge at the PH2 geometry.

As described in the introduction, the two different geometries for $M_3C_{60}^+$ and $M_3C_{60}^-$ are speculated from the

Table 6. The adsorption energies ΔE (in eV) and the Mulliken charges per alkali atom (in electrons) of M_3C_{60}.

	P3		H3		tP3		tH3		PH2	
	ΔE	Charge	ΔE	Charge	ΔE	Charge	ΔE	Charge	ΔE	Charge
$Li_3C_{60}^-$	6.090	+0.800	5.976	+0.808	6.180	+0.705	5.884	+0.749	5.503	+0.593
$Na_3C_{60}^-$	4.362	+0.951	4.155	+0.971	3.910	+0.851	3.659	+0.828	3.847	+0.512
$K_3C_{60}^-$	4.254	+0.971	4.622	+1.009	3.756	+0.759	4.052	+0.831	3.960*	+0.583*

* Geometry is nearly converged.

results of experiments. A speculated geometry is a trimer on C_{60} caused by special stability of a singly positive charged alkali trimer in which the two valence electrons occupy the bonding orbital of the alkali atom. Since the distance between the alkali atoms in the PH2 geometry is similar as the twice of the atomic radius of the alkali atom, the *s*-dominant bonding orbital of M_3C_{60} is expected to be occupied for the PH2 geometry. The calculated results show that the *s*-dominant bonding orbital is occupied but is strongly mixed with the molecular orbital mostly composed of the carbon atomic orbital. The total Mulliken charges of the alkali trimer for the PH2 geometry is calculated as (+1.5)–(+1.8). The remaining 1.2–1.5 valence electrons in the alkali trimer may be small to stabilize the PH2 geometry compared with the other geometries. In fact, the adsorption energy of the PH2 geometry of the alkali atoms are at least 0.5 eV higher than that of the most stable geometry.

The Mulliken charge of the alkali atoms for M_3C_{60} and $M_3C_{60}^+$ are higher than that of $M_3C_{60}^-$. Then, the bonding between the alkali atoms is expected to be less attractive in M_3C_{60} and $M_3C_{60}^+$. Therefore, we conclude that the repulsive Coulomb interaction is still dominant for $M_3C_{60}^q$ ($q = 0, \pm 1$). A trimer on fullerene speculated by the experiments is not the most stable geometry in our calculation.

3.2.4 $M_{12}C_{60}$

Two types of initial geometries considered for $M_{12}C_{60}$ are P12 and 4PH2 which are illustrated in Figure 6d. The initial positions of the alkali atoms are located above the twelve pentagonal rings for the P12 geometry. In the 4PH2 geometry, the alkali atoms form four trimers on the C_{60} surface. One of the atoms in the trimer is located above the pentagonal ring and the others are located above the adjacent hexagonal rings.

The adsorption energies and the Mulliken charges for $M_{12}C_{60}$ are tabulated in Table 7. The Mulliken charges of the alkali atoms of the P12 geometry are larger than those of the 4PH2 geometry for all kinds of alkali atoms. The most stable geometry is the 4PH2 geometry for $Na_{12}C_{60}$ and $K_{12}C_{60}$. The adsorption energy for the 4PH2 geometry is about 1–2 eV higher than that of the P12 geometry. The result is consistent with the speculation from the experiment, that is, the metal-metal bond in the Na atoms on C_{60} appears for more than the 6 valence electrons in Na_xC_{60}. On the other hand, the P12 geometry is the most stable geometry for $Li_{12}C_{60}$. This result agrees with the density functional study by Kohanoff in which the geometry of $Li_{12}C_{60}$ is optimized using the Car-Parrinello method [9].

Table 7. The adsorption energies ΔE (in eV) and the Mulliken charges per alkali atom (in electrons) of $M_{12}C_{60}$.

	P12		4PH2	
	ΔE	Charge	ΔE	Charge
$Li_{12}C_{60}$	25.15	+0.547	22.35	+0.514
$Na_{12}C_{60}$	15.96	+0.570	18.04	+0.466
$K_{12}C_{60}$	17.30	+0.568	18.64	+0.525

4 Summary and conclusion

We have performed the LDA calculations with the LCAO approach to study the bonding nature of a single alkali atom to C_{60} and the bonding between many alkali atoms on C_{60}. The Mulliken charge of an alkali atom is determined for MC_{60} of the five types of initial geometries. The results of Mulliken charges lying between +0.8 and +1.1 for all kinds of alkali atoms indicate the ionic bond between a single alkali atom and C_{60}. The increase of the Mulliken charge of the alkali atom from lithium to potassium is originated from the increase of the valence orbital energy of the alkali atom. The dipole moment evaluated for MC_{60} agrees with the experimental result. The difference between the calculated adsorption energies for the five types of geometries are less than 1.0 eV. The maximum of adsorption energy obtained at the P1 or the H1 geometry indicate that the alkali atom prefers to make many bonds with the neighbor carbon atoms rather than a single strong bond with a single carbon atom.

The Mulliken charge per alkali atom for M_xC_{60} is evaluated in the present calculation. The decrease of the Mulliken charge for larger number of the alkali atoms indicates the increase of covalency between the alkali atoms and C_{60}. We find, in the present calculation, that the Mulliken charge of lithium is smaller than that of the other alkali atoms. The result reflects the more covalent character of the lithium-carbon interaction relative to the other alkali atoms, which is also true in the alkali-graphite intercalation compounds [24] and organolithium

compounds [25]. The covalent character of lithium is originated from the character of the lithium atom, such as higher polarlizability, more diffuse valence orbitals, and lower energy of the valence p orbitals, compared with those of the other alkali atoms.

We find from the calculated adsorption energy of $M_xC_{60}^q$ for $(x,q) = (6,-1),(12,0)$ that the most stable geometry is different between lithium and the other alkali atoms for more than the six valence electrons in the alkali atoms. The most stable geometries for potassiums and sodiums on C_{60} are the PH5 and the 4PH2 geometry, while for lithiums, the P6 and the P12 geometry are the most stable geometries. The results support the speculation for bonding of $M_xC_{60}^+$ by Martin *et al.* in which the Na–Na bonding appears for $Na_xC_{60}^+$ molecules having more than the 6 valence electrons. On the other hand, there are no significant differences between the most stable geometry of lithium and the other alkali atoms for $M_xC_{60}^q$, $(x,q) = (2,0),(3,-1),(6,0)$. The most stable geometries are P2, H2, P3, H3, P6, and 2P3 in which one alkali atom is adsorbed on C_{60} away from another alkali atom. A single trimer on C_{60} can not be regarded as the most stable geometry in our calculation.

As presented in Figure 7, the energy of the s-dominant bonding orbital is lower than that of the t_{1g} orbital in Na_6C_{60} and K_6C_{60}. On the other hand, is higher in Li_6C_{60}. For sodium and potassium, the s-dominant bonding orbital is occupied if the number of the valence electrons is larger than six. The electrons in the s-dominant bonding orbital weakens the metal-carbon bond, while arises the covalent bonding between the alkali atoms. The potassium and the sodium atoms, therefore, prefers to be located in close positions together like the PH5 and the 4PH2 geometry. On the other hand, for lithium, the s-dominant bonding orbital is not occupied for the number of electrons larger than six. The lithium atoms are, therefore, located far from each other in the most stable geometry such as the alkali atoms in the P6 and the P12 geometry. When the number of valence electrons is smaller than seven, the s-dominant bonding orbital of the alkali atom is not occupied. The alkali atoms, therefore, prefers to be located far from each other like the alkali atoms in P2, H2, P3, H3, P6, and 2P3.

The differences of the most stable geometry between $Li_6C_{60}^-$ and $Na_6C_{60}^-$, $K_6C_{60}^-$ are explained by the position of the t_{1g} orbital in Figure 7, that is, the t_{1g} level of Li_6C_{60} located lower than the s-dominant bonding orbital is shifted to the higher position than the s-dominant bonding orbital in Na_6C_{60} and K_6C_{60}. The t_{1g} orbital energy shift is explained by the charge transfer from the alkali atom to C_{60}, in other words, the covalency of the metal-carbon interaction. Therefore, $Li_6C_{60}^-$ prefers the covalent lithium-carbon bonding rather than the metal-metal bonding, while $Na_6C_{60}^-$ and $K_6C_{60}^-$ prefers the metal-metal bonding.

Since the Mulliken charges for M_xC_{60} (x = 7–11) are considered to be smaller than those of M_6C_{60}, the metal-metal interaction will be less repulsive. Therefore, Na_xC_{60} and K_xC_{60} (x = 7–11) will prefer the metal-metal bond. For Li_xC_{60} (x = 7–11), although the decrease of the Coulomb interaction reduces the metal-metal repulsive interaction, $Li_{12}C_{60}$ still prefers the metal-carbon bonding. Li_xC_{60} (x = 7–11) is, therefore, expected to prefer the metal-carbon bond. For M_xC_{60} ($x < 6$), the Mulliken charges are higher than those of M_6C_{60}, which causes the stronger Coulomb repulsion. In the most stable geometry, the alkali atoms on C_{60} will be placed themselves as far from one another as possible.

In this work, we assumed that the positions of the carbon atom in C_{60} are not changed in the geometry optimization. Although the assumption is justified by comparing the full geometry optimization calculation of NaC_{60}^- and the result of our calculation, the assumption might not be justified for the other M_xC_{60} molecules. We believe, however, that the results of the bonding nature of M_xC_{60} are not changed for the full geometry optimization calculation. Performing the full geometry optimization calculation is the subject of the further study.

One of the authors (N.H.) acknowledges a financial support from a Grant from the Ministry of Education, Science, Sports and Culture to promote advanced scientific research. This work is financially supported by a Grant-in-Aid in the area "Physics and Chemistry of Molecules" (Grant No. 11166261) from Ministry of Education, Science, Sports, and Culture of Japan.

References

1. A.F. Hebard, M.J. Rosseinsky, R.C. Haddon, D.W. Murphy, S.H. Glarum, T.T.M. Palstra, A.P. Ramirez, A.R. Kortan, Nature **350**, 600 (1991).
2. K. Holczer, O. Klein, S.-M. Huang, R.B. Kaner, K.-J. Fu, R.L. Whetten, F. Diederich, Science **252**, 1154 (1991).
3. T.P. Martin, N. Malinowski, U. Zimmermann, U. Näher, H. Schaber, J. Chem. Phys. **99**, 4210 (1993).
4. B. Palpant, A. Otake, F. Hayakawa, Y. Negishi, G.H. Lee, A. Nakajima, K. Kaya, Phys. Rev. B **60**, 4509 (1999).
5. B. Palpant, Y. Negishi, M. Sanekata, K. Miyajima, S. Nagao, K. Judai, D.M. Rayner, B. Simard, P.A. Hackett, A. Nakajima, K. Kaya, J. Chem. Phys. **114**, 8549 (2001).
6. L.-S. Wang, O. Cheshnovsky, R.E. Smalley, J.P. Carpenter, S.J. Hwu, J. Chem. Phys. **96**, 4028 (1992).
7. D. Östling, A. Rosén, Chem. Phys. Lett. **281**, 352 (1997).
8. D. Östling, A. Rosén, Chem. Phys. Lett. **202**, 389 (1993).
9. J. Kohanoff, W. Andreoni, M. Parrinello, Chem. Phys. Lett. **198**, 472 (1992).
10. T. Aree, T. Kerdcharoen, S. Hannongbua, Chem. Phys. Lett. **285**, 221 (1998).
11. T. Aree, S. Hannongbua, J. Phys. Chem. A **101**, 5551 (1997).
12. A.S. Hira, A.K. Ray, Phys. Rev. A **52**, 141 (1995).
13. A.S. Hira, A.K. Ray, Phys. Rev. A **54**, 2205 (1996).
14. P. Weis, R.D. Beck, G. Bräuchle, M.M. Kappes, J. Chem. Phys. **100**, 5684 (1994).
15. U. Zimmermann, A. Burkhardt, N. Malinowski, U. Näher, T.P. Martin, J. Chem. Phys. **101**, 2244 (1994).

16. E.J. Baerends, D.E. Ellis, P. Ros, Chem. Phys. **2**, 41 (1973); L. Versluis, T. Ziegler, J. Chem. Phys. **322**, 88 (1988); G. te Velde, E.J. Baerends, J. Comput. Phys. **99** (1), 84 (1992); C.F. Guerra, J.G. Snijders, G. te Velde, E.J. Baerends, Theor. Chem. Acc. **99**, 391 (1998); Eur. Phys. J. D **12**, 147 (2000).
17. S.H. Vosko, L. Wilk, M. Nusair, Can. J. Phys. **58**, 1200 (1980).
18. K. Hedberg, L. Hedberg, D.S. Bethune, C.A. Brown, H.C. Dorn, R.D. Johnson, M. de Vries, Science **254**, 410 (1991).
19. M. Häser, J. Almlöf, G.E. Scuseria, Chem. Phys. Lett. **181**, 497 (1991).
20. S.H. Yang, C.L. Pettiette, J. Conceicao, O. Cheshnovsky, R.E. Smalley, Chem. Phys. Lett. **139**, 233 (1987).
21. R.S. Mulliken, J. Chem. Phys. **23**, 1833 (1955).
22. D. Rayane, R. Antoine, Ph. Dugourd, E. Benichou, A.R. Allouche, M. Aubert-Frécon, M. Broyer, Phys. Rev. Lett. **84**, 1962 (2000).
23. R. Antoine, D. Rayane, E. Benichou, Ph. Dugourd, M. Broyer, Eur. Phys. J. D **12**, 147 (2000).
24. C. Hartwigsen, W. Witschel, E. Spohr, Phys. Rev. B **55**, 4953 (1997).
25. A. Streitwieser, S.M. Bachrach, A. Dorigo, P.v.R. Schleyer, in *Lithium Chemistry: A Theoretical and Experimental Overview*, edited by A.-M. Sapse, P.v.R. Schleyer (Wiley, New York, 1995).
26. R.R. Teachout, R.T. Pack, Atom. Data **3**, 195 (1971).
27. C. Kittel, *Introduction to solid state physics* (Wiley, New York, 1986).